Proc. Natl. Acad. Sci. USA
Vol. 93, pp. 6258–6263, June 1996
Medical Sciences

Fatal embryonic bleeding events in mice lacking tissue factor, the cell-associated initiator of blood coagulation

(gene targeting/embryonic development)

THOMAS H. BUGGE*†, QING XIAO*, KEITH W. KOMBRINCK*, MATTHEW J. FLICK*, KENN HOLMBÄCK*, MARY JO S. DANTON*, MELISSA C. COLBERT‡, DAVID P. WITTE§, KAZUO FUJIKAWA¶, EARL W. DAVIE¶, AND JAY L. DEGEN*‖

Divisions of *Developmental Biology, ‡Molecular Cardiovascular Biology, and §Pathology, Children's Hospital Research Foundation, Cincinnati, OH 45229; †Finsen Laboratory, Rigshospitalet, DK-2100 Copenhagen 0, Denmark; and ¶Department of Biochemistry, University of Washington, Seattle, WA 98195

Contributed by Earl W. Davie, February 29, 1996

ABSTRACT **Tissue factor (TF) is the cellular receptor for coagulation factor VII/VIIa and is the membrane-bound glycoprotein that is generally viewed as the primary physiological initiator of blood coagulation. To define in greater detail the physiological role of TF in development and hemostasis, the TF gene was disrupted in mice. Mice heterozygous for the inactivated TF allele expressed approximately half the TF activity of wild-type mice but were phenotypically normal. However, homozygous $TF^{-/-}$ pups were never born in crosses between heterozygous mice. Analysis of mid-gestation embryos showed that $TF^{-/-}$ embryos die *in utero* between days 8.5 and 10.5. $TF^{-/-}$ embryos were morphologically distinct from their $TF^{+/+}$ and $TF^{+/-}$ littermates after day 9.5 in that they were pale, edematous, and growth retarded. Histological studies showed that early organogenesis was normal. The initial failure in $TF^{-/-}$ embryos appeared to be hemorrhaging, leading to the leakage of embryonic red cells from both extraembryonic and embryonic vessels. These studies indicate that TF plays an indispensable role in establishing and/or maintaining vascular integrity in the developing embryo at a time when embryonic and extraembryonic vasculatures are fusing and blood circulation begins.**

Tissue factor (TF) is a 47-kDa membrane-bound glycoprotein that functions as the cellular receptor for coagulation factor VII/VIIa. TF is thought to be the primary physiological initiator of blood coagulation following vascular damage (1). Unlike other coagulation factors, TF need not be activated and is delivered to the cell surface as a functional VII/VIIa receptor. Factor VIIa bound to TF at the cell surface efficiently catalyzes the proteolytic activation of coagulation factors IX and X. This ultimately leads to local thrombin generation and thrombin-catalyzed events such as fibrin formation and the activation of factors V, VIII, XIII, thrombin receptor, and protein C (1).

The central role of TF in blood coagulation *in vivo* is supported by several compelling, but indirect, observations. First, severe congenital deficiencies in factor VII can produce bleeding problems similar to classic hemophilias (2). Second, TF-deficient patients have never been identified, suggesting that TF deficiency may be lethal due to a coagulation disorder. Finally, the normal distribution of TF *in vivo* is consistent with the view that TF provides a hemostatic "envelope" outside of the vasculature that will initiate local coagulation in the event of vessel rupture (3).

Although TF is best understood in the context of hemostasis, the physiological and pathological roles of TF may not be restricted to the initiation of blood coagulation. Notably, the angiogenic or metastatic properties of experimental tumor models have frequently been shown to depend on TF (4, 5), but the biological properties of these tumor cells does not always appear to depend on factor VII binding or other coagulation pathway components (5). For example, the metastatic potential of one human melanoma cell line has recently been shown to depend on sequences in the cytoplasmic domain of TF and not on factor VII binding or procoagulant activity (5). A role of TF outside of hemostasis is also implied by the number and diversity of cytokines, growth factors, hormones, and hormone-like agents that are known to regulate TF gene expression (6).

To rigorously define the physiological role of TF in development and hemostasis, we have disrupted the TF gene in mice. We report that TF-deficient embryos die *in utero* between embryonic days 8.5 and 10.5. The lethal phenotype appears to be result from the massive hemorrhaging of embryonic blood from both extraembryonic and embryonic vessels.

MATERIALS AND METHODS

Generation of TF-Deficient Mice. The arms of the TF targeting vector were generated by PCR using oligonucleotide primers complementary to mouse TF gene sequences (7) and 129/SvJ tail biopsy DNA as a template. For the short arm (see Fig. 1*A*), we used primers that were complementary to 5′-flanking sequences and that correspond to positions −982 to −957 and −283 to −258 in the gene sequence (TFP-5′, 5′-ATCAGAATGCGGCCGCGCTACCAGTAGGATAAGTGATCGTCT-3′; TFP-3′, 5′-TTACGCGTCGACCGGATCCAGGTACTGCGGAGACCCAG-3′). These primers were designed with *Not*I (TFP-5′) and *Sal*I (TFP-3′) sites to facilitate the cloning of the PCR product into the plasmid vector, Bluescript II (Stratagene). For the long arm (see Fig. 1*A*), primers complementary to the sequences within exons 3 and 5 were generated (TF3–5′, 5′-TTACGCGTCGACGGTCCTCTCTGTCCCACGGAGGAACT-3′; TF5–3′, 5′-ATCAATGGTACCCCACATCAATCGAGAATTCATTGGTG-3′). These primers were designed with *Sal*I (TF3–5′) and *Kpn*I (TF5–3′) sites to assist in the cloning of the PCR product. A 3.2-kb PGK-HPRT minigene cassette (8) was inserted into the *Sal*I site between the short and long arms in the opposite transcriptional orientation as the TF gene. A herpes simplex virus thymidine kinase (HSV-tk) gene was inserted into a *Kpn*I site adjacent to the TF gene sequences to provide a means to select against transfectants integrating the targeting vector by nonhomologous recombination (9). The targeting vector was linearized with *Not*I and introduced into embryonic stem (ES)

The publication costs of this article were defrayed in part by page charge payment. This article must therefore be hereby marked "*advertisement*" in accordance with 18 U.S.C. §1734 solely to indicate this fact.

Abbreviations: TF, tissue factor; HSV-tk; herpes simplex virus thymidine kinase; ES, embryonic stem; HPRT, hypoxanthine phosphoribosyltransferase.

‖To whom reprint requests should be addressed at: Children's Hospital Research Foundation, Children's Hospital Medical Center, TCHRF Room 2025, 3333 Burnet Avenue, Cincinnati, OH 45229-3039.

cell line E14TG2a by electroporation (10). Stable transfectants were selected in hypoxanthine/aminopterin/thymidine medium containing 2 μM ganciclovir as described (10). DNA extracts were prepared from clonal isolates and tested for the presence of the targeted TF allele by a PCR assay using the diagnostic oligonucleotide primers TFES (5′-GGATAAACTGGACAGTCAACCAGGAGTGACAAG-3′) and PGKpolyA (5′-CCTGAAGAACGAGATCAGCAGCCTCTGTTC-3′). The TFES primer corresponds to a TF gene sequence located upstream of the short arm of the targeting vector (positions −1043 to −1011 relative to the TF transcription initiation site; ref. 7), and the PGKpolyA primer corresponds to a sequence in the HPRT cassette. These primers give rise to an 878-bp PCR product with DNA from correctly targeted cells. PCR-positive clones were injected into C57BL/6-derived blastocysts, and these were subsequently implanted into pseudopregnant females to generate chimeric mice (10). Chimeric offspring were mated to NIH Black Swiss mice (Taconic Farms), and tail biopsy DNAs from agouti offspring were tested for the targeted TF allele using the TFES and PGKpolyA primers described above. As an additional, independent test for the correct targeting of the TF gene, tail biopsy DNAs were assayed using the oligonucleotide primers TFE5 (5′-TCACCTCCCAGGAATCTTCCATTG-3′) and HPRT#2 (5′-GTGCGAGGCCAGAGGCCACTTGTGTAGCG-3′). The TFE5 primer is complementary to a sequence in the mouse TF gene that spans the exon 5–intron 5 junction, a sequence downstream of the long arm of the targeting vector (7). Primer TFE5 in combination with HPRT minigene primer HPRT#2 yields a 3.3-kb PCR product with DNA preparations from targeted cells.

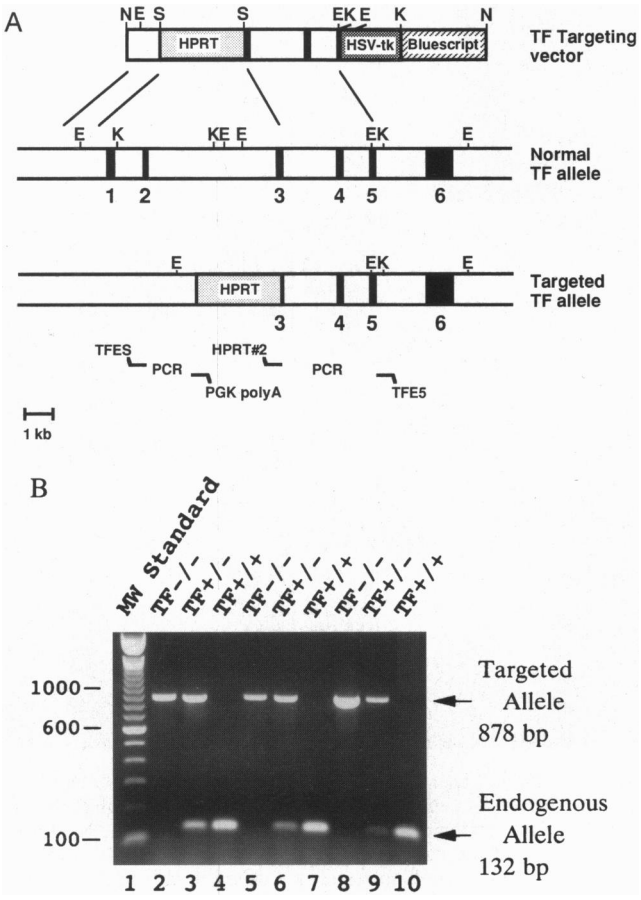

FIG. 1. Targeting of the murine TF gene. (*A*) Structure of the TF targeting vector, the normal mouse TF gene (7), and targeted TF gene. Solid bars indicate the position of exons (numbered 1 through 6). The 3.2-kb HPRT and 2.0 kb HSV-tk minigenes that were introduced into the targeting vector as selectable markers are shown as shaded regions. The relative positions of the PCR oligonucleotide primers used for the initial screening of ES cell clones and to document the presence of the targeted TF allele in transgenic mice are shown at bottom. E, *Eco*RI; K, *Kpn*I; S, *Sal*I; N, *Not*I. (*B*) Representative data obtained in multiplex PCR analysis of individual, day 9.5 yolk sac DNA extracts using the primers TFES and PGKpolyA to detect the targeted TF allele and TFEX2–5′ and TFEX2–3′ to detect the normal TF allele.

Genotype Analysis of the Offspring of Heterozygous Breeding Pairs. Progeny were genotyped by multiplex PCR analysis using DNA extracts prepared from tail biopsies, embryos, or yolk sacs. The presence of the mutant TF allele was detected using the PGKpolyA primer (see above) and a primer complementary to a 5′-flanking sequence of the TF gene, TFP5′-2 (5′-ACTGCGTGTTCAGGCAGGGCTTTGGAACTG-3′; nucleotides −491 to −462 in the gene sequence; ref. 7), which yield a 326-bp product. The normal TF allele was detected using primers complementary to the intron 1–exon 2 junction (TFEX2–5′; 5′-TGCTTATTTGTAGGCATTCCAGAGAAAGCG-3′) and the exon 2–intron 2 junction (TFEX2–3′; 5′-TAACCTGGCTTACCTTATCTGTACAGTGTA-3′). Primers TFEX2–5′ and TFEX2–3′ give rise to a 132-bp product only with the normal allele.

Histological Analysis of Mice. Tissues were fixed in either buffered 10% formalin (Sigma) or Bouin fixative (Poly Scientific), processed into paraffin, sectioned, and stained with hematoxylin/eosin.

Hematological Analysis and Bleeding Time Measurements. Blood collection, blood cell counts, plasma thrombin times, and bleeding times following a standard nail bed incision were determined as described (11).

TF Activity in Tissue Extracts. Whole brain and lung samples from wild-type and heterozygous mice were homogenized in 25 ml of 50 mM Bis-Tris, pH 7.4/50 mM NaCl, and the homogenates were centrifuged at 40,000 rpm for 1 hr. The pelleted material was resuspended in approximately 10 ml of extraction buffer for brain samples and 2 ml of extraction buffer for lung samples. Clotting activity was assayed in samples serially diluted over a 2.5- to 20-fold range (three dilutions). Test samples (40 μl) were placed in siliconized tubes, mixed with 40 μl of normal mouse plasma, and warmed to 37°C, and clotting times were recorded after the addition of 80 μl of stock rabbit brain cephalin (prepared by suspending an entire vial of cephalin (Sigma) in 100 ml of buffered saline, then adding an equal volume of 40 mM $CaCl_2$). The units of clotting activity were calculated from a standard curve using normal brain and lung extracts. The standard curve was linear from 20 to 45 sec. The specific activity of each sample was obtained by adjusting for the protein concentration (Pierce BCA assay).

RESULTS

Disruption of the TF Gene. To inactivate the TF gene in mice, a replacement-type targeting vector was constructed

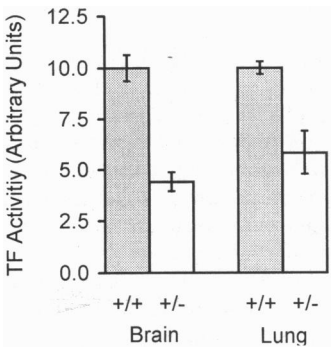

FIG. 2. TF activity in tissue extracts from adult $TF^{+/+}$ and $TF^{+/-}$ mice. TF activities were determined by partial thromboplastin time clotting assays using five independent brain, and four independent lung, microsome preparations from mice of each genotype. The average activity in preparations from $TF^{+/+}$ mice was defined arbitrarily as 10 units.

Table 1. Genotypes of the progeny from heterozygous matings

Stage	No. of litters	No. of offspring	No. of resorptions	No. of pups typed	TF genotype +/+	TF genotype +/−	TF genotype −/−
E9.5	5	56	4	50	10 (20)	24 (48)	16 (32)
E10.5	3	32	0	32	5 (16)	19 (59)	8 (25)
E11.5	1	12	1	11	5 (45)	6 (55)	0 (0)
E12.5	2	18	3	14	3 (21)	11 (79)	0 (0)
E15.5	4	37	8	29	11 (38)	18 (62)	0 (0)
P0–P22	16	79	NA	79	30 (38)	49 (62)	0 (0)

E, embryonic day; P, postnatal day; NA, not applicable; +/+, wild type; +/−, heterozygotes; −/−, homozygotes. Number in parentheses indicates the percentage of typed offspring.

(Fig. 1*A*). The vector contained a 725-bp fragment from the 5′-flanking region of the mouse TF gene and an approximately 3.2-kb fragment from the region spanning exons 3 through 5. Integration of the targeting vector into the mouse genome by homologous recombination results in the deletion of a 6-kb fragment, including the proximal promoter region, transcriptional start site, exon 1 (encoding the signal peptide), exon 2, and part of exon 3 (encoding most of the first immunoglobulin-like extracellular domain). The targeting vector was introduced into the HPRT-deficient ES cell line E14TG2a, and 2 of 89 clones tested positive for the targeted TF gene by PCR analysis of genomic DNA (data not shown). Mice were raised from the targeted ES cells and shown to transmit the targeted allele to their offspring by two independent PCR strategies (see *Materials and Methods*). Heterozygous, $TF^{+/-}$, mice were crossed to generate offspring that were genotyped either in mid-gestation or shortly after birth (see Fig. 1 and below).

Characterization of $TF^{+/-}$ Mice. Heterozygous mice appeared outwardly normal, exhibited normal weight gain, and could produce and sustain multiple litters. The body weights of young adult $TF^{+/-}$ and $TF^{+/+}$ mice (8–13 weeks of age) were 29.9 ± 4.8 g (n = 10) and 31.3 ± 2.6 g (n = 12), respectively. $TF^{+/+}$ and $TF^{+/-}$ mice were also indistinguishable with regard to platelet, red cell and white cell counts, hematocrit, thrombin-initiated plasma clotting time, and bleeding time after a surgical nail bed challenge (data not shown). Furthermore, a microscopic survey of tissues collected from five adult (11- to 13-week-old) $TF^{+/-}$ mice did not reveal abnormalities in any major organ system (data not shown). However, based on the level of TF clotting activity in brain and lung microsome preparations, $TF^{+/-}$ mice could be readily distinguished from $TF^{+/+}$ mice (Fig. 2). The average TF clotting activity in microsome preparations from $TF^{+/-}$ was approximately half of that observed in similar preparations from $TF^{+/+}$ mice. These results clearly show that TF expression in mice depends on gene dosage and that mice can cope with half-normal TF activity, even in the face of an injury.

TF Deficiency Is Embryonic-Lethal. Crosses between $TF^{+/-}$ mice did not result in any viable $TF^{-/-}$ progeny. Of 79 mice that were born from heterozygous breeding pairs, 49 (62%) were found to be $TF^{+/-}$, 30 (38%) were identified as homozygous $TF^{+/+}$, and none were homozygous $TF^{-/-}$ (Table 1). The ≈2:1 ratio of $TF^{+/-}$ and $TF^{+/+}$ mice in term offspring suggests that there were no significant losses of heterozygous mice *in utero*.

To rigorously determine whether TF deficiency results in an embryonic-lethal phenotype, embryos were collected from timed matings between $TF^{+/-}$ mice and then genotyped by PCR analysis of either yolk sac or embryo DNA (representative examples shown in Fig. 1*B*). Beyond embryonic day 11.5, only $TF^{+/-}$ and $TF^{+/+}$ embryos were found, together with partially resorbed remains that could not be genotyped (Table 1). However, at embryonic day 10.5 and earlier, $TF^{-/-}$ embryos were present and the ratio of $TF^{-/-}$, $TF^{+/-}$, and $TF^{+/+}$ embryos closely followed the pattern expected for a Mendelian transmission of the mutant TF allele (Table 1).

TF Deficiency Results in Embryonic Hemorrhaging. Day 10.5 $TF^{-/-}$ embryos where immediately distinguishable from their $TF^{+/-}$ and $TF^{+/+}$ littermates based on the extreme pallor of both the yolk sac and the embryo itself (Fig. 3). In addition, pools of red blood cells, later shown to be nucleated embryonic red cells (see below), were often observed macroscopically within the $TF^{-/-}$ yolk sac cavities (Fig. 3 *B* and *C*). A branching

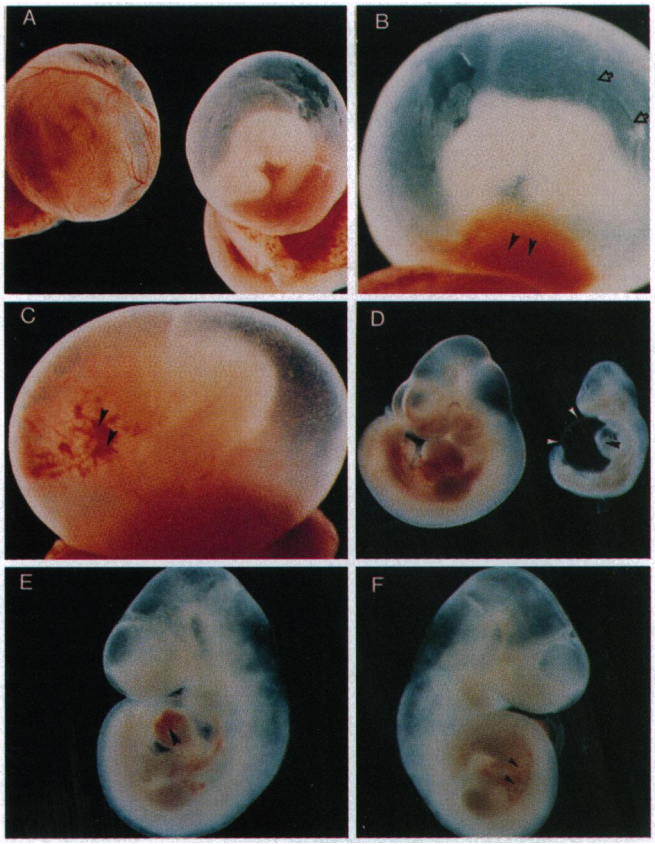

FIG. 3. Gross appearance of day 9.5 and day 10.5 $TF^{-/-}$ embryos. (*A*) Day 10.5 $TF^{+/-}$ (left) and $TF^{-/-}$ (right) embryos within their yolk sacs. Note the extreme pallor of the mutant embryo. (*B*) Higher magnification of the day 10.5 $TF^{-/-}$ embryo shown in *A*. Note that large and branching vitelline vessels are clearly visible in the yolk sac (open arrows). Also note the large pool of red cells that has spilled into the yolk sac cavity (filled arrowheads). (*C*) Another example of a day 10.5 $TF^{-/-}$ embryo with the typical pale appearance and free blood within the yolk sac cavity. (*D*) Day 10.5 $TF^{+/+}$ (left) and $TF^{-/-}$ (right) embryos dissected from their yolk sacs. Note the obvious developmental arrest, pale appearance, massively enlarged pericardial sac (white arrow heads), and distended heart (black arrowhead) of the mutant embryo. (*E*) Day 9.5 $TF^{-/-}$ embryo with pale appearance, enlarged pericardial sac, and poorly developed prosencephalon. Note that red cells are visible within the heart (arrowhead). (*F*) The opposite side of same day 9.5 $TF^{-/-}$ embryo shown in *E*. Note that some red cells are macroscopically visible in the caudal portion of the embryo (arrowheads).

vascular plexus was apparently present in $TF^{-/-}$ yolk sacs, but the vessels appeared empty (Fig. 3 *B* and *C*). Day 10.5 $TF^{-/-}$ embryos were considerably smaller than their $TF^{+/-}$ and $TF^{+/+}$ littermates, and most had extremely enlarged pericardial sacs and distended hearts (Fig. 3*D*). Despite obvious embryonic growth retardation, cardiac contractions were observed in several day 10.5 $TF^{-/-}$ embryos. Day 9.5 $TF^{-/-}$ embryos were variable with regard to overt abnormalities; 3 of 16 examined appeared morphologically unremarkable, whereas the remaining 13 were clearly abnormal, with extremely pale yolk sacs, highly enlarged pericardial sacs, poorly developed forebrain structures, and aplasia (Fig. 3 *E* and *F*). In spite of these overt defects, some aspects of early development proceeded normally in many $TF^{-/-}$ embryos, such as formation of branchial arches, otic vesicles, and early forelimb buds (Fig. 3 *E* and *F*). Day 8.5 $TF^{-/-}$ embryos were indistinguishable from $TF^{+/-}$ and $TF^{+/+}$ littermates both macroscopically and microscopically (data not shown).

Histological analyses of day 9.5 $TF^{-/-}$ embryos consistently revealed very few embryonic (nucleated) red cells within the yolk sac (vitelline), embryonic, and placental vasculatures (Figs. 4 *B* and *D* and 5 *B*, *C*, and *E*). This lack of red cells was not due to a wholesale failure in either vessel formation or yolk sac hematopoiesis. Well-formed vasculatures with appropriate endothelial linings were evident in both extraembryonic tissues (e.g., placenta and yolk sac; Fig. 4 *B* and *D*) and embryonic tissues (Fig. 5 *B*, *C*, and *E*). Furthermore, fetal blood cells were always present in the day 8.5 yolk sac membranes and, while scarce, could also be found in occasional embryonic and placental vasculature of day 9.5 $TF^{-/-}$ embryos (Figs. 4 and 5). The most obvious and impressive developmental failure in day 9.5 $TF^{-/-}$ embryos was the massive spillage of embryonic red cells into the yolk sac cavity (see representative example in Fig. 5 *B* and *C*). The loss of vascular integrity was not confined to extraembryonic tissues; leakage of red cells into the pericardial sac was frequently noted in mutant embryos (for examples, see Fig. 5 *B* and *E*). This blood loss appears to be an early, if not the initial, failure in $TF^{-/-}$ embryos in that some typically hemorrhagic day 9.5 embryos had sustained little or no tissue necrosis (see Fig. 5 *B*, *C*, and *F*). However, the extent of tissue necrosis varied widely among day 9.5 $TF^{-/-}$ embryos, from slight (Fig. 5 *B*, *C*, and *F*) to widespread (Fig. 5*G*). On day 10.5, tissue necrosis in $TF^{-/-}$ embryos was consistently severe (a representative example is shown in Fig. 5*I*). Thus, the data suggest that the initial developmental failure in $TF^{-/-}$ embryos occurs after day 8.5 and before day 9.5, the period in which yolk sac vasculogenesis is completed, the extraembryonic and embryonic vasculatures are fused, and embryonic blood circulation begins. Further, the data suggest that a catastrophic loss of vascular integrity in $TF^{-/-}$ embryos, particularly in extraembryonic tissues, leads to developmental arrest, progressive ischemic necrosis, and ultimately, death.

DISCUSSION

This study demonstrates that TF plays a crucial role in early embryonic development. TF deficiency is uniformly lethal *in utero* with developmental arrest occurring between embryonic days 8.5 and 9.5. The initial failure appears to be, or coincides with, hemorrhaging into the yolk sac cavity. Other phenotypic properties, such as pericardial sac enlargement and nonspecific tissue necrosis, are most likely secondary consequences of the failure to establish sufficient circulating blood cells to maintain rapid embryonic growth (see below). Consistent with this view, several day 9.5 $TF^{-/-}$ embryos that had sustained massive hemorrhages into their yolk sacs exhibited no other obvious developmental abnormalities other than small foci of necrosis (for example, see Fig. 5*B*). Thus, the major conclusion drawn from this study is that TF plays an indispensable role in establishing and/or maintaining vascular integrity in the developing embryo at a time when embryonic and extraembryonic vasculatures are initially forming and fusing. A number of hypotheses can be imagined for the mechanism by which TF expression might preserve vascular integrity, but the simplest hypothesis is surely that, as in mature animals, TF initiates local thrombin generation and fibrin deposition at the points of vascular damage and rupture (see further discussion below).

Extraembryonic vessels are almost certainly the source of the pooled blood found within the yolk sac cavities of day 9.5 $TF^{-/-}$ embryos. This is inferred from the fact that only trace amounts of free blood were detected within mutant embryos and none was detected within amniotic sacs. However, the critical event or events that lead to bleeding around day 9 and the precise sources of free-blood remain open questions. There are two major events in the development of the extraembryonic vasculature that occur around the time that $TF^{-/-}$ embryos hemorrhage, and one or both events may lead to bleeding in the absence of TF. One of these events is the fusion of blood islands within the visceral yolk sac to form the yolk sac vascular system that links to the embryo via the vitelline

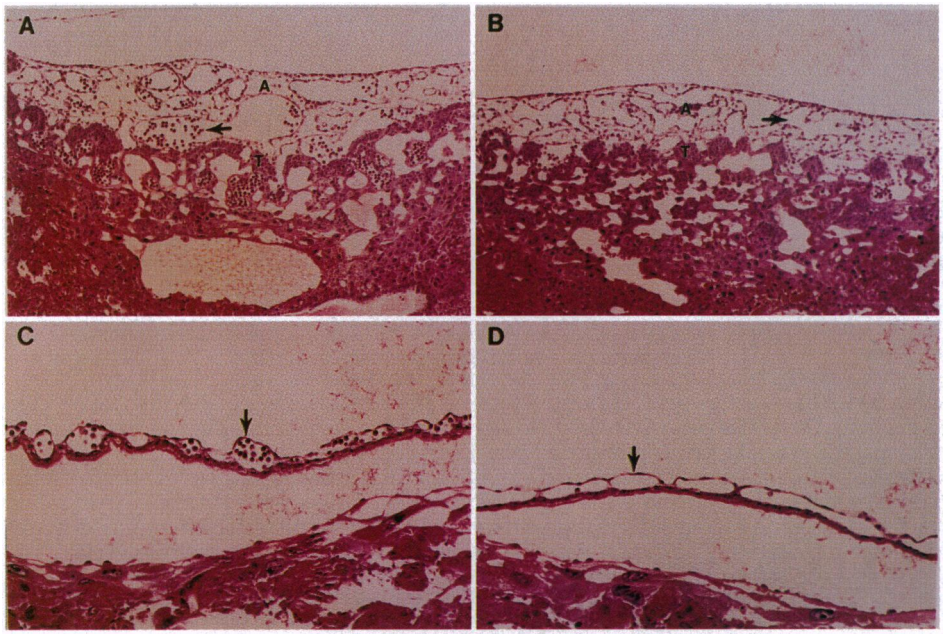

FIG. 4. Microscopic analysis of the placenta and yolk sac of $TF^{-/-}$ embryos. (*A*) Representative section through the placenta of a normal day 9.5 embryo. Note the high density of nucleated embryonic blood cells that stain darkly in allantoic vessels (arrow) and developing labryinthine region. A, allantois; T, trophectoderm. (*B*) Representative section through the placenta of a day 9.5 $TF^{-/-}$ embryo. The placenta contains very few embryonic red cells, but the vessels of the allantois and developing labryinthine layer appear to be well-formed (arrow). A, allantois; T, trophectoderm. (*C*) Representative section through the yolk sac of a normal day 9.5 embryo. Red cells are densely packed within the yolk sac vasculature (arrow). (*D*) Representative section through the yolk sac of a day 9.5 $TF^{-/-}$ embryo. The yolk sac vessels appear well-formed but they are nearly devoid of red cells.

artery and veins. The second is the fusion of the allantois with the chorion leading to the establishment of vascular connections between both the embryo and the placenta via the umbilical artery and veins. A hemorrhagic risk may be an inherent feature of the fusion of blood islands to form primitive capillaries and/or the subsequent fusion of capillaries to form a highly branched plexus of vessels. The risk may be even more substantial in the fusion of the umbilical vessels with the newly established placental vasculature. Nevertheless, there is evidence that $TF^{-/-}$ embryos have at least partial success with each of these key developmental milestones. The visceral yolk sac mesoderm cells of $TF^{-/-}$ embryos clearly differentiate into both endothelial cells and hematopoietic cells, and these organize into well-formed blood islands and, ultimately, into macroscopically visible, but largely empty, vitelline vessels. In addition, the allantois of $TF^{-/-}$ embryos fuses with the chorionic plate, creating vascular conduits that allow at least a few red cells to pass from the yolk sac to the embryo and then on to the placenta. However, our working hypothesis is that the integrity of newly formed extraembryonic vessels and/or their newly established junctions may be easily compromised in the absence of TF. This leads to massive extraembryonic bleeding before substantial blood cell infusion from the yolk sac into the embryo. This model does not exclude the possibility that TF is also critical for vascular integrity elsewhere in the embryo. Indeed, the occasional finding of free blood within pericardial sacs of day 9.5 $TF^{-/-}$ embryos is consistent with a more general role of TF in either establishing or preserving embryonic vascular integrity.

Yolk sac abnormalities associated with an embryonic-lethal phenotype around day 10 have been documented with many

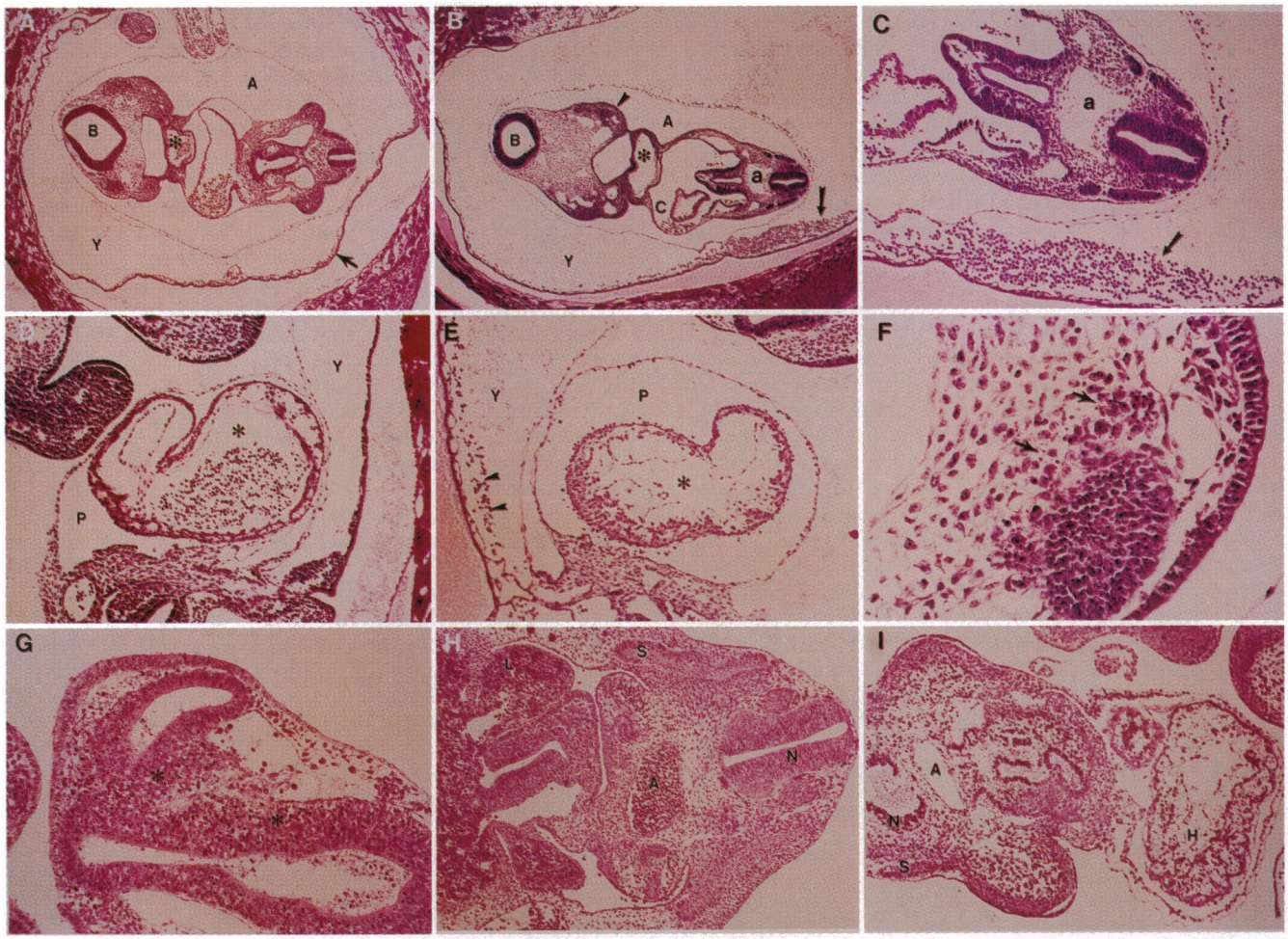

FIG. 5. Microscopic analysis of day 9.5 and day 10.5 embryos. (*A*) Section of a normal day 9.5 embryo within the decidua. Note that embryonic red cells are densely packed within the vascular spaces of the embryo and yolk sac membrane. Y, yolk sac cavity; A, amniotic space; B, brain; asterisk, branchial artery; arrow, yolk sac membrane. (*B*) Section through a mutant day 9.5 embryo oriented similarly to the embryo shown in *A*. Note the general scarcity of embryonic red cells within the vascular spaces of the embryo and yolk sac membrane. The branchial artery and aorta are nearly devoid of red cells. This embryo exhibits the hemorrhagic phenotype typical of $TF^{-/-}$ embryos with obvious extraembryonic bleeding into the yolk sac cavity (large arrow) and embryonic bleeding into the coelomic cavity. The hemorrhagic failure in this embryo would appear to have been a recent event in that only small foci of tissue necrosis are apparent (see higher magnification of region marked by arrowhead in *F*). Y, yolk sac cavity; A, amniotic space; B, brain; C, coelomic cavity; a, aorta; asterisk, branchial artery; large arrow, yolk sac membrane; arrowhead, small foci of necrosis. (*C*) Higher magnification of the embryo shown in *B* showing absence of red cells within the aorta (a) and a substantial quantity of free blood in the yolk sac cavity (arrow). (*D*) High magnification view of a normal day 9.5 embryo showing the heart. Note that red cells are densely packed within the cardiac ventricular cavity (asterisk) but not found within the pericardial sac (P), adjacent coelomic cavity, or yolk sac cavity (Y). (*E*) High magnification view of a mutant day 9.5 embryo oriented similarly to the embryo shown in *D*. Note the extremely enlarged pericardial sac (P) containing free red cells, and the free blood (arrows) in the yolk sac cavity (Y). The heart (asterisk) contains the expected epicardial, myocardial, and endocardial layers. (*F*) High magnification view of the necrotic area highlighted by an arrowhead in *B*. Scattered pycnotic nuclei are indicated by arrows. (*G*) High magnification view of the head region of a day 9.5 $TF^{-/-}$ embryo illustrating that severe ischemic necrosis could be found in mutant embryos at this gestational age. Necrotic neuroepithelial layer of the forebrain is indicated by asterisk. (*H*) High magnification view of a portion of a normal day 10.5 embryo. N, neural tube; S, somite; L, liver; A, aorta. (*I*) High magnification view of a mutant day 10.5 embryo showing massive nonspecific necrosis. N, neural tube; S, somite; H, heart; A, aorta.

genes previously targeted in mice, including the genes encoding transforming growth factor $\beta 1$, integrin subunit α_5, the tyrosine kinase receptors for vascular endothelial growth factor (*flk-1* and *flt-1*), and several hematopoietic transcription factors (*scl/tal-1*, *rbtn-2*, and GATA-2) (12–19). Like $TF^{-/-}$ mice, embryos deficient in transforming growth factor $\beta 1$, integrin α_5, *flk-1*, *flt-1*, *scl/tal-1*, *rbtn-2*, and GATA-2 showed no obvious abnormalities before day 9.5, and beyond day 9.5, all of these mutants exhibit a grossly anemic appearance, enlarged pericardial sacs, and growth retardation. However, microscopically, the $TF^{-/-}$ mice are clearly distinct from these other knock-out mice, which exhibit either disorganized vessels, lack of vessels, impaired hematopoiesis, or a combination of these disorders. In contrast, $TF^{-/-}$ embryos develop well-formed vessels and produce hematopoietic cells but, nevertheless, uniformly develop a catastrophic hemorrhagic failure.

One of the most interesting aspects of the finding that TF deficiency results in a hemorrhagic, embryonic-lethal phenotype is that the loss of another key hemostatic factor, fibrinogen, does not result in an embryonic-lethal phenotype (11). Based on this fact, one might argue that if TF plays an essential role in maintaining embryonic vascular integrity, then the critical function of TF must not be in directing local fibrin formation. However, given that fibrinogen-deficient ($A\alpha$ $chain^{-/-}$) embryos were shown to survive to term only when carried by $A\alpha$ $chain^{+/-}$ mothers, the possibility that maternally derived fibrinogen "rescues" mid-gestation $A\alpha^{-/-}$ embryos was never formally eliminated (11). Mid-gestation embryogenesis may depend on a functional coagulation system that is based in part on access to maternally derived coagulation factors. An implicit extension of this hypothesis is that non-circulating, cell-associated coagulation factors that cannot be acquired from the maternal circulation, such as TF and thrombomodulin, would be indispensable for embryonic development. Notably, thrombomodulin deficiency in mice was recently shown to be fatal *in utero*, with the first embryonic abnormalities occurring between day 7.5 and 8.5 (20, 21).

Direct studies of fibrin deposition in the extraembryonic tissues of control and $TF^{-/-}$ embryos would be useful in establishing any linkage between TF and fibrinogen in maintaining embryonic vascular integrity. Interestingly, fibrin(ogen) has been observed in extraembryonic tissues before day 8.5 in normal embryos and found to increase in the absence of the coagulation suppressor, thrombomodulin (21). Therefore, it appears that early embryos do have a source of fibrinogen (either embryonic or maternal) and perhaps other soluble coagulation factors. If controlled coagulation is critical to preserve vascular integrity in extraembryonic vessels, then inappropriate fibrin deposition leading to compromised vascular patency would provide one explanation for the lethal phenotype of thrombomodulin-deficient mice (20, 21).

We thank Terry Smith and Kathy Saalfeld for technical assistance. This work was supported by National Institutes of Health Grants HL47826 (to J.L.D.) and HL16919 (to E.W.D.) and American Heart Association Ohio Affiliate Grant SW 95-29-1 (to D.P.W.). This study was done during the tenure of an Established Investigatorship (J.L.D.) from the American Heart Association (93002570). T.H.B. and K.H. were supported by grants from the Danish Medical Research Council.

1. Davie, E. W., Fujikawa, K. & Kisiel, W. (1991) *Biochemistry* **30,** 10363–10370.
2. Triplett, D. A. (1984) *Clin. Lab. Med.* **4,** 221–244.
3. Drake, T. A., Morrissey, J. H. & Edgington, T. S. (1989) *Am. J. Pathol.* **134,** 1087–1097.
4. Mueller, B. M., Reisfeld, R. A., Edgington, T. S. & Ruf, T. (1992) *Proc. Natl. Acad. Sci. USA* **89,** 11832–11836.
5. Bromberg, M. E., Konigsberg, W. H., Madison, J. F., Pawashe, A. & Garen, A. (1995) *Proc. Natl. Acad. Sci. USA* **92,** 8205–8209.
6. Mackman, N. (1995) *FASEB J.* **9,** 883–889.
7. Mackman, N., Imes, S., Maske, W. H., Taylor, B., Lusis, A. J. & Drake, T. A. (1992) *Arterioscler. Thromb.* **12,** 474–483.
8. van der Lugt, N., Maandag, E. R., teRiele, H., Laird, P. W. & Berns, A. (1991) *Gene* **105,** 263–267.
9. Mansour, S. L., Thomas, K. R. & Capecchi, M. R. (1988) *Nature (London)* **336,** 348–352.
10. Bugge, T. H., Flick, M. J., Daugherty, C. C. & Degen, J. L. (1995) *Genes Dev.* **9,** 794–807.
11. Suh, T. T., Holmbäck, K., Jensen, N. J., Daugherty, C. C., Small, K., Simon, D. I., Potter, S. S. & Degen, J. L. *Genes Dev.* **9,** 2020–2033.
12. Dickson, M. C., Martin, J. S., Cousins, F. M., Kulkarni, A. B., Karlsson, S. & Akhurst, R. J. (1995) *Development* **121,** 1845–1854.
13. Yang, J. T., Rayburn, H. & Hynes, R. O. (1993) *Development* **119,** 1093–1105.
14. Shalaby, F., Rossant, J., Yamaguchi, T. P., Gertsenstein, M., Wu, X.-F., Breitman, M. L. & Schuh, A. C. (1995) *Nature (London)* **376,** 62–66.
15. Fong, G.-H., Rossant, J., Gertsenstein, M. & Breitman, M. L. (1995) *Nature (London)* **376,** 66–70.
16. Robb, L., Lyons, I., Li, R., Hartley, L., Köntgen, F., Harvey, R. P., Metcalf, D. & Begley, C. G. (1995) *Proc. Natl. Acad. Sci. USA* **92,** 7075–7079.
17. Shivdasani, R. A., Mayer, E. L. & Orkin, S. H. (1995) *Nature (London)* **373,** 432–434.
18. Warren, A. J., Colledge, W. H., Carlton, M. B. L., Evans, M. J., Smith, A. J. H. & Rabbits, T. H. (1994) *Cell* **78,** 45–57.
19. Tsai, F.-Y., Keller, G., Kuo, F. C., Weiss, M., Chen, J., Rosenblatt, M., Alt, F. W. & Orkin, S. H. (1994) *Nature (London)* **371,** 221–226.
20. Healy, A. M., Rayburn, H. B., Rosenberg, R. D. & Weiler, H. (1995) *Proc. Natl. Acad. Sci. USA* **92,** 850–854.
21. Rosenberg, R. D. (1995) *Thromb. Haemostasis* **74,** 52–57.